doi:10.1016/j.jmb.2003.11.044 J. Mol. Biol. (2004) 336, 473–487

JMB

Available online at www.sciencedirect.com

SCIENCE DIRECT®

ELSEVIER

Crystal Structure of a cAMP-dependent Protein Kinase Mutant at 1.26 Å: New Insights into the Catalytic Mechanism

Jie Yang[1], Lynn F. Ten Eyck[2,3], Nguyen-Huu Xuong[2,4] and Susan S. Taylor[1,2]*

[1]*Howard Hughes Medical Institute, University of California San Diego, 9500 Gilman Drive, La Jolla, CA 92093, USA*

[2]*Department of Chemistry and Biochemistry, University of California San Diego, 9500 Gilman Drive, La Jolla, CA 92093, USA*

[3]*Department of Pharmacology the San Diego Supercomputer Center, University of California San Diego, 9500 Gilman Drive La Jolla, CA 92093, USA*

[4]*Department of Physics University of California San Diego, 9500 Gilman Drive, La Jolla, CA 92093, USA*

**Corresponding author*

The catalytic subunit of cAMP-dependent protein kinase has served as a paradigm for the entire kinase family. In the course of studying the structure–function relationship of the P + 1 loop (Leu198–Leu205) of the kinase, we have solved the crystal structure of the Tyr204 to Ala mutant in complexes with Mg·ATP and an inhibitory peptide at 1.26 Å, with overall structure very similar to that of the wild-type protein. However, at the nucleotide binding site, ATP was found largely hydrolyzed, with the products ADP-PO_4 retained in the structure. High-resolution refinement suggests that 26% of the molecules contain the intact ATP, whereas 74% have the hydrolyzed products. The observation of the substrate and product states in the same structure adds significant information to our understanding of the phosphoryl transfer process. Structural examination of the mutation site substantiates and extends the emerging concept that the hydrophobic core in the large lobe of the kinase might serve as a stable platform for anchoring key segments involved in catalysis. We propose that Tyr204 is critical for anchoring the P + 1 loop to the core. Further analysis has highlighted two major connections between the P + 1 loop and the catalytic loop (Arg165–Asn171). One emphasizes the hydrophobic packing of Tyr204 and Leu167 mediated through residues from the αF-helix, recently recognized as a signal integration motif, which together with the αE-helix forms the center of the hydrophobic core network. The other connection is mediated by the hydrogen bond interaction between Thr201 and Asp166, in a substrate-dependent manner. We speculate that the latter interaction may be important for the kinase to sense the presence of substrate and prepare itself for the catalytic reaction. Thus, the P + 1 loop is not merely involved in substrate binding; it mediates the communication between substrate and catalytic residues.

Keywords: crystal structure; cAMP-dependent protein kinase; catalytic mechanism; P + 1 loop; hydrophobic core

Introduction

The catalytic subunit of cAMP-dependent protein kinase (PKAc) has served as a prototype and provided significant insights for many kinases from both structure–function relationship and catalytic mechanism points of view.[1–3] Through extensive investigations utilizing a wide variety of methods, much is known about this enzyme in terms of its catalytic mechanism and its interaction with regulatory subunits, protein inhibitors and substrates.[4] Crystal structures of PKAc in complexes with substrate/inhibitory peptides and various nucleotides/analogs have provided a series of snapshots that enabled us to have a good understanding of interactions between the enzyme

Abbreviations used: cAMP, adenosine 3′,5′-cyclic monophosphate; PKAc, the catalytic subunit of cAMP-dependent protein kinase; Y204A, the Tyr204 to Ala mutant of PKAc; IP20, a 20-mer inhibitory peptide of PKAc; SP20, a 20-mer substrate peptide for PKAc; RMSD, root-mean-squared deviation; MPD, 2-methyl-2,4-pentanediol.

E-mail address of the corresponding author: staylor@ucsd.edu

and the substrates at different stages along the reaction pathway.[5–9] These include the ternary complex of PKAc with Mn·ATP and a 20-mer inhibitory peptide IP20 (PKAc:Mn·ATP:IP20, PDB ID 1ATP),[8] which represents the reactant stage, and the transition state mimic structure where PKAc was complexed with Mg·ADP, aluminum fluoride and a 20-mer substrate peptide SP20 (PKAc:Mg·ADP·AlF_3:SP20, PDB ID 1L3R).[5] Complementary biophysical methods such as fluorescence anisotropy and hydrogen/deuterium exchange coupled with mass spectrometry have, on the other hand, provided significant insight into and greatly promoted our appreciation of the dynamic aspects of the enzyme.[4]

The PKAc structure defines the prototype of the bilobal kinase-like fold[10,11] that is characterized by a small lobe with mainly β-sheet structure and a large lobe of mainly α-helices. The interface of the two lobes forms the wedge-shaped active-site cleft with the sharp end close to the hinge region. Sensing the occupancy of nucleotide and peptide substrate, the active site toggles between an ensemble of open and closed conformations achieved by the relative motion between the two lobes. The opening and closure of the active-site cleft is essential for catalysis and thus constitutes an important part of the catalytic cycle. The large lobe is centered by two interacting hydrophobic helices, designated as αE and αF. Extensive hydrophobic interactions radiate through the whole large lobe, making it a very stable substructure. The αF-helix has been proposed to function as a signal integration motif, partly because of its connection with the catalytic loop.[4] Analysis of the very recently reported structure of unliganded PKAc apo-enzyme has suggested that the hydrophobic core may mediate the synergistic binding of the nucleotide and the peptide substrates. Roles of the hydrophobic core as a platform for anchoring catalytic residues and a communication center have been proposed.[12]

As reviewed extensively, clusters of conserved residues in the kinase families identified by sequence alignment map well to three-dimensional segments that are also structurally conserved.[2,13] For example, the glycine-rich motif GXGXXG (in single-letter amino acid code) folds into a β-hairpin (Gly50–Gly55 in PKAc) connecting two β-strands in the small lobe of the kinase core, and constitutes a major part of the nucleotide-binding pocket. The conformation of this loop is sensitive to which form of nucleotide occupies the pocket. The catalytic loop (Arg165–Asn171 in PKAc) harbors residues that are involved directly in catalysis; and the activation loop (Arg192–Thr197 in PKAc) contains the highly conserved Thr197, whose phosphorylation is required for an active enzyme in the arginine-aspartate (R-D) family of kinases.[14] In PKAc, the segment immediately after the activation loop is the P + 1 loop, including residues Leu198–Leu205. The consensus PKAc phosphorylation site has been defined as (R)XXRRXS/TΦ, where S/T is the phosphate acceptor, referred as the P-site, and Φ represents a hydrophobic residue. Leu198, Pro202 and Leu205 form a hydrophobic pocket to accommodate the hydrophobic side-chain of the residue at the P + 1 site, whereas the carbonyl oxygen atom of Gly200 is within hydrogen bond distance of its backbone amide group. Glu203 interacts with the arginine residue at the P − 6 position, and the Tyr204 hydroxyl moiety is within hydrogen bond distance of the Glu230 side-chain that has important ionic interaction with the P − 2 arginine residue. The P + 1 loop is named as the peptide-positioning loop because of its multiple contacts with the protein substrate. While many studies have been conducted on dissecting other functioning motifs or residues, little has been done on the P + 1 loop, since its function appeared obvious and simple. However, very recent mutagenesis analysis has revealed unexpected results; the P + 1 loop mutants exhibited a significantly decreased catalytic turnover rate k_{cat}.[15] In particular, the Tyr204 to Ala mutation (Y204A) caused a tenfold increase in K_m, and a 30-fold decrease in k_{cat}, when using kemptide as substrate.[15] While it is not hard to rationalize the alteration in K_m, the reason for the decreased k_{cat} is not immediately clear.

Essential for a diversity of cellular functions, PKAc has evolved into a very sophisticated and "sensitive" molecule, capable of responding to differential regulations through communication between its different parts. For example, mutagenesis studies have shown that mutation of residues distal to the phosphoryl transfer site can affect the kinetic properties of the enzyme,[16] and mutations on the nucleotide-binding glycine-rich loop can affect the binding constant for the substrate peptide.[17] Similar observations have been made on other molecules, and theoretical work by Ranganathan *et al.* has identified such connection pathways.[18,19] These studies depict an extensive network of interaction within the molecule, and have emphasized that each part of the molecule is connected to other parts at a higher level of organization. Tyr204 is not in the active site, yet its mutation results in a dramatic decrease in phosphoryl transfer rate. To have a better understanding of the P + 1 loop and the mechanism behind the altered catalytic properties of the mutant, we solved the crystal structure of the Y204A mutant at 1.26 Å resolution. Structural analysis has suggested a role of Tyr204 in anchoring the P + 1 loop to the hydrophobic core in the large lobe and highlighted two major connections between the P + 1 loop and the catalytic loop. The dynamic effect of disrupting the P + 1 loop by the Tyr204 to Ala mutation can be transmitted to the catalytic loop to affect the catalytic properties of the enzyme. In addition, possibly due to the altered properties of the mutant, we unexpectedly observe coexistence of ATP and its hydrolyzed products ADP-PO_4 in different molecules of the same

crystal. This enables the investigation of the whole catalytic process in more detail.

Results

Overall structure

The ternary structure of Y204A in complex with Mg·ATP (see below for detail) and IP20 was solved at 1.26 Å resolution with crystallographic *R*-factor of 13.2% and R_{free} of 16.2% (Table 1). Its overall structure was very similar to that of the closed form of the wild-type protein ternary complex such as PKAc:Mn·ATP:IP20 (1ATP).[8] Least-squares superimposition of the C^{α} atoms of residues 15–350 of these two structures resulted in a root-mean-square deviation of 0.4 Å. Interactions between the protein molecule and Mg·ATP or IP20, or important contacts within the protein molecule[20] were largely preserved in the mutant structure.

The very N terminus of PKAc is highly mobile and usually unresolved in the crystal structure.[10,21] It was barely traceable in the structure of the *N*-myristylated protein.[22,23] In the current low-temperature structure, however, clear electron density was observed for the first four or five residues (Figure 1a). This N-terminal piece was anchored near the hinge region in the small lobe through direct or indirect (mediated by a water molecule) hydrogen bond interactions with several residues from the loop connecting the αC-helix and β4-strand (Asn99, Pro101, Leu103, Lys105 and Glu107), Tyr306 and Arg308 from a stable short helix, and Gln181 (Figure 1b and c). Its location was apparently different from that in the myristylated protein, where the myristic acid moiety was bound at a hydrophobic groove in the large lobe.[22,23] An MPD molecule from the crystallization solution was found occupying the groove in some of the non-myristylated PKAc structures (1L3R, 1J3H), including the current one (Figure 1b). This N-terminal piece was observed in the recently solved structure of PKAc:Mg·ADP·AlF_3:SP20 (1L3R),[5] suggesting its presence was not due to the mutation. This is the first detailed structural description of the very N terminus of the non-myristylated protein. Its docking site could be a plausible interface for other PKAc-interacting proteins. Note this N terminus is close to one end of the αC-helix, where its other end provides the docking site for the hydrophobic motif at the very C terminus (FTEF) of the protein (Figure 1c). Studies on other AGC family kinases, protein kinase B/Akt and 3-phosphoinositide-dependent protein kinase 1, have shown that the interaction with the conserved FXXF motif is important for stabilizing/positioning the αC-helix in the conformation associated with the active enzyme.[24–27]

Table 1. Data collection and refinement statistics

Resolution (Å)	50.00–1.26
Mosaicity	0.22
Completeness (%)	94.1 (61.0)
I/σ	19.7 (3.4)
R_{merge} [a]	0.045 (0.253)
Space group	$P2_12_12_1$
a (Å)	57.76
b (Å)	79.51
c (Å)	97.74
R_{cryst}/R_{free} [b]	13.2/16.2
RMSD bond (Å)	0.006
RMSD angle (deg.)	1.812

Values in parentheses are for high-resolution shells, 1.26–1.28 Å.

[a] $R_{merge} = \sum_{hkl}|I - \langle I\rangle|/\sum\langle I\rangle$, is the mean intensity for the symmetry-equivalent reflections.

[b] $R_{cryst} = \sum_{hkl}|F_o| - |F_c|)/\sum|F_o|$, R_{free} is calculated on 5% of the data omitted by random.

Two nucleotide states and active-site conformation

Although the crystallization was set up in the presence of ATP, the triphosphate nucleotide was found mostly hydrolyzed in the crystal of Y204A, as suggested by the ATP-omit map (Figure 2a). Several lines of evidence indicated the presence of a small portion of non-cleaved ATP; the most apparent one was the bulge (indicated by arrow) in the density of the leaving phosphate group (Figure 2a). Refinement of ATP as the only nucleotide gave a very elongated bond between the β-γ bridging oxygen atom and the γ-phosphorus atom (see Materials and Methods), and residual density where an attacking water oxygen atom would be placed. Refinement of ADP and PO_4 as the only nucleotide left residual density between the ADP and PO_4 groups. Modeling bound nucleotide as a mixture of ATP and ADP-PO_4 gave a clean residual map. This caused a decrease in both *R* and R_{free} by 0.15%, as compared with that when ATP was modeled. Refinement suggested occupancy of 0.26 and 0.74 for ATP and ADP-PO_4, respectively. The ADP moiety of ATP superimposed almost identically with ADP in the hydrolyzed molecule (Figure 2c).

Despite the coexistence of pre- and post-phosphoryl transfer molecules, active-site residues exhibited unambiguous single conformations (Figure 2b) with very low temperature factors. In contrast, Ser53, a residue located at the tip of the glycine-rich loop, clearly showed double conformations for its side-chain, as indicated from the electron density map (Figure 2b). Conformation A (occupancy of 0.6) was at a position similar to that observed in the previous ternary structures, while in conformation B (occupancy of 0.4), the O^{γ} atom was 1.4 Å away and toward the phosphate group (Figure 2c). When assuming conformation B, the O^{γ} of Ser53 was within hydrogen-bond distance with the oxygen atom from the γ-phosphate group or the free phosphate group and, interestingly, the backbone amide group of the

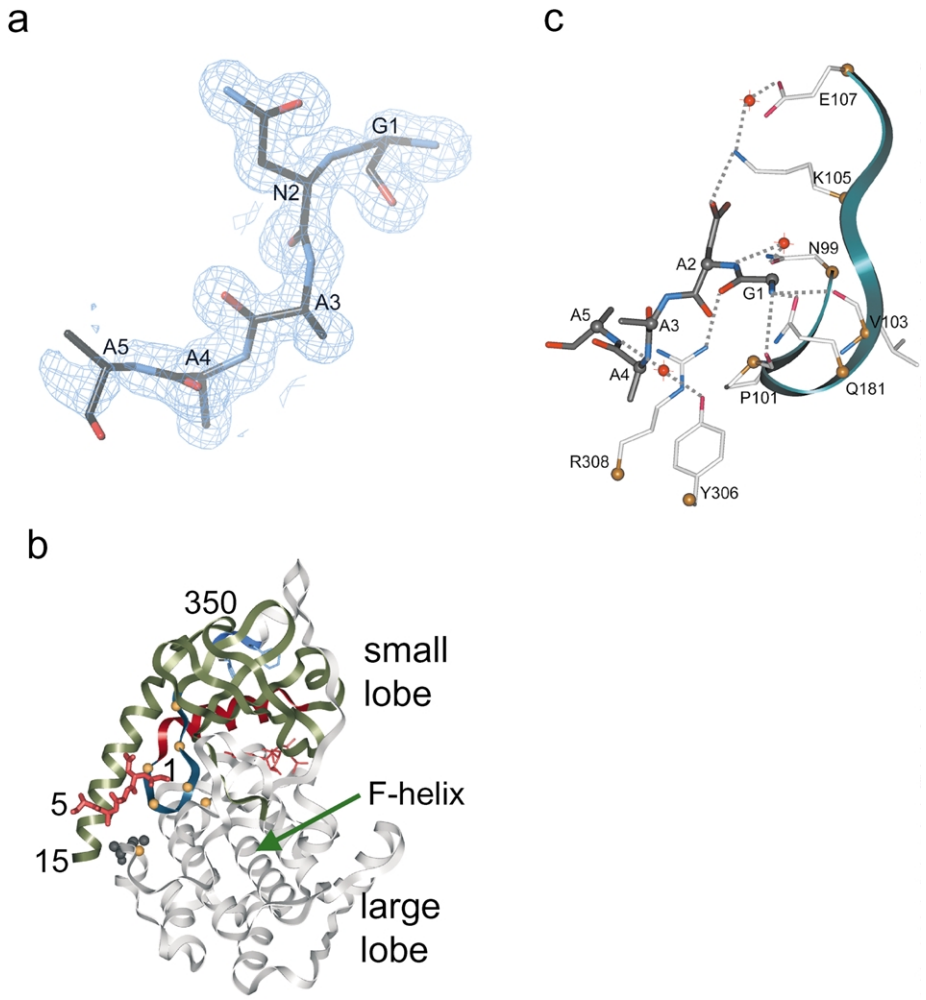

Figure 1. The N terminus (residues 1–5) of PKAc. a, Electron density map of the first five residues. The $2F_o - F_c$ map is contoured at the 1σ level. The model of residues 1–5 is shown as colored sticks, with carbon atoms gray, nitrogen atoms blue and oxygen atoms red. b, Ribbon diagram of the overall structure of Y204A showing the N terminus binding site relative to the myristic acid binding groove. The C-helix is colored in red. The trace of the C terminus FTEF motif including the two Phe residues is shown in blue. ATP is shown in red. The αC–β4 loop that participates in binding is shown in dark green. The C^{α} atoms of the interacting residues are highlighted in golden spheres. The myristic acid binding groove is filled by an MPD molecule shown in gray spheres. c, Close-up of the interaction between the N terminus and its binding site in the small lobe. Dotted lines indicate the possible hydrogen bonding interactions. Residues are labeled with the single-letter amino acid code. The C^{α} atoms of the residues are rendered as spheres. Water molecules are shown as red spheres.

P-site residue (Figure 2c). It is possible that conformation A dominated in the ground state, whereas conformation B was present only in the transition state. In the current structure, due to the special environment, where the active site remained closed and contracted after phosphoryl transfer had been completed, some ADP-PO_4-containing molecule may retain some transition-state "memory", keeping Ser53 in conformation B. That is probably why only 40% of the molecules were in this conformation, while 76% had already completed the reaction.

The interactions of active-site residues with ATP were similar to those in the wild-type structure (1ATP) (Figure 3a). Most residues interacting with the γ-phosphate group of ATP "followed" it to the product state and formed similar interactions with the free PO_4 (Figure 3a and b). The free phosphate was in a position similar to that of the AlF_3 in the transition state mimic structure (1L3R) (Figure 3b). The deviation between PO_4:O4, coming from the attacking water molecule, and the hydroxyl group of Ser377, the phosphoacceptor serine residue in SP20 (1L3R), was only 0.2 Å, implying that the phosphoacceptor was at a similar position before and after reaction. It appeared that only the γ-phosphate group "traveled" toward the attacking water molecule to form the product PO_4. Figure 3c compares the interactions between active-site residues and the γ-phosphate group of ATP (current structure), free phosphate (current structure) or transition-state analog AlF_3 (1L3R). In all cases, either the phosphate groups or AlF_3 was within hydrogen bond distance from the backbond

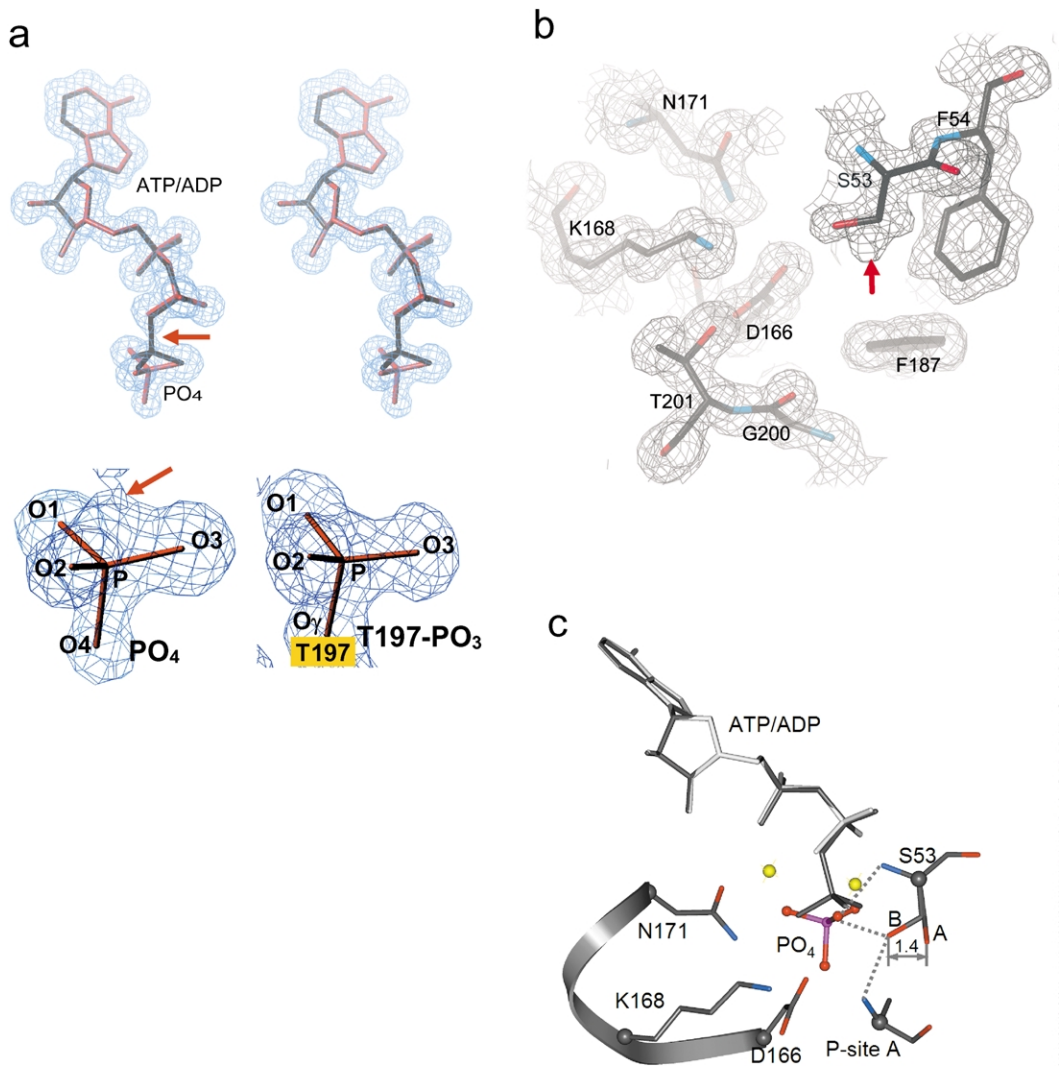

Figure 2. Two nucleotide states in the crystal. a, Upper, a composite sigmaA-weighted $F_o - F_c$, map omitting the nucleotide was contoured at the 3σ level. Both ATP (black sticks) and ADP-PO_4 (red sticks) are modeled to fit the density. The arrow indicates the "bulge" density that should not be present if ATP is fully hydrolyzed. Lower left, a $2F_o - F_c$ (1σ) map with ADP-PO_4 modeled, focused on the bulge region shown above. For comparison, the density for a completely cleaved phosphate group is shown (lower right), which is exemplified by the phosphate group transferred to Thr197. b, Double conformation of the Ser53 side-chain. The $2F_o - F_c$ map is contoured at the 1σ level. The arrow indicates the electron density for the second possible conformation of the Ser53 side-chain. c, Active site with partial occupancy of ATP and ADP-PO_4. ATP is shown in black sticks and ADP in gray. PO_4 is shown as ball-and-stick with the phosphorus atom colored in magenta and oxygen atoms in red. Two conformations of the Ser53 side-chain are labeled as A and B; the distance between the side-chain hydroxyl groups is indicated. All atoms in Ser53 and P-site Ala521 but only C^{α} and side-chains for Asp166, N171 and Lys168 are shown. C^{α} atoms are rendered as gray spheres. The two magnesium ions are shown as yellow spheres.

amide group of Ser53, the N^{ζ} atom of Lys168, and the oxygen atoms of two water molecules. They were further stabilized by coordinating with the two metal ions. Conformation B of Ser53 is unique to the current structure. The distance between O^{γ} of Ser53 and one of the oxygen atoms from the γ-phosphate group or the free phosphate group was ~2.5 Å. The interaction with Asn171 is strengthened in both AlF_3 and free phosphate state, as compared with that in the ATP state. The distance from the γ-phosphate oxygen atom to $N^{\delta 2}$ of Ans171 was 3.7 Å in the ATP state, but 3.3 Å and 3.1 Å, respectively, from the free phosphate and AlF_3.

Inhibition of ATPase activity by IP20

Earlier studies have shown that PKAc exhibited very low intrinsic ATPase activity that could be fully abolished by IP20.[28] Thus in the ternary complex of wild-type protein, what we have been seeing was the unhydrolyzed ATP. Observing ATP hydrolysis in the Y204A crystal was unexpected. To understand how the hydrolysis could occur, we compared the ATPase activities of the mutant and the wild-type enzymes and their inhibition by IP20. Consistent with the previous data,[28] our assay showed that the ATPase activity for the

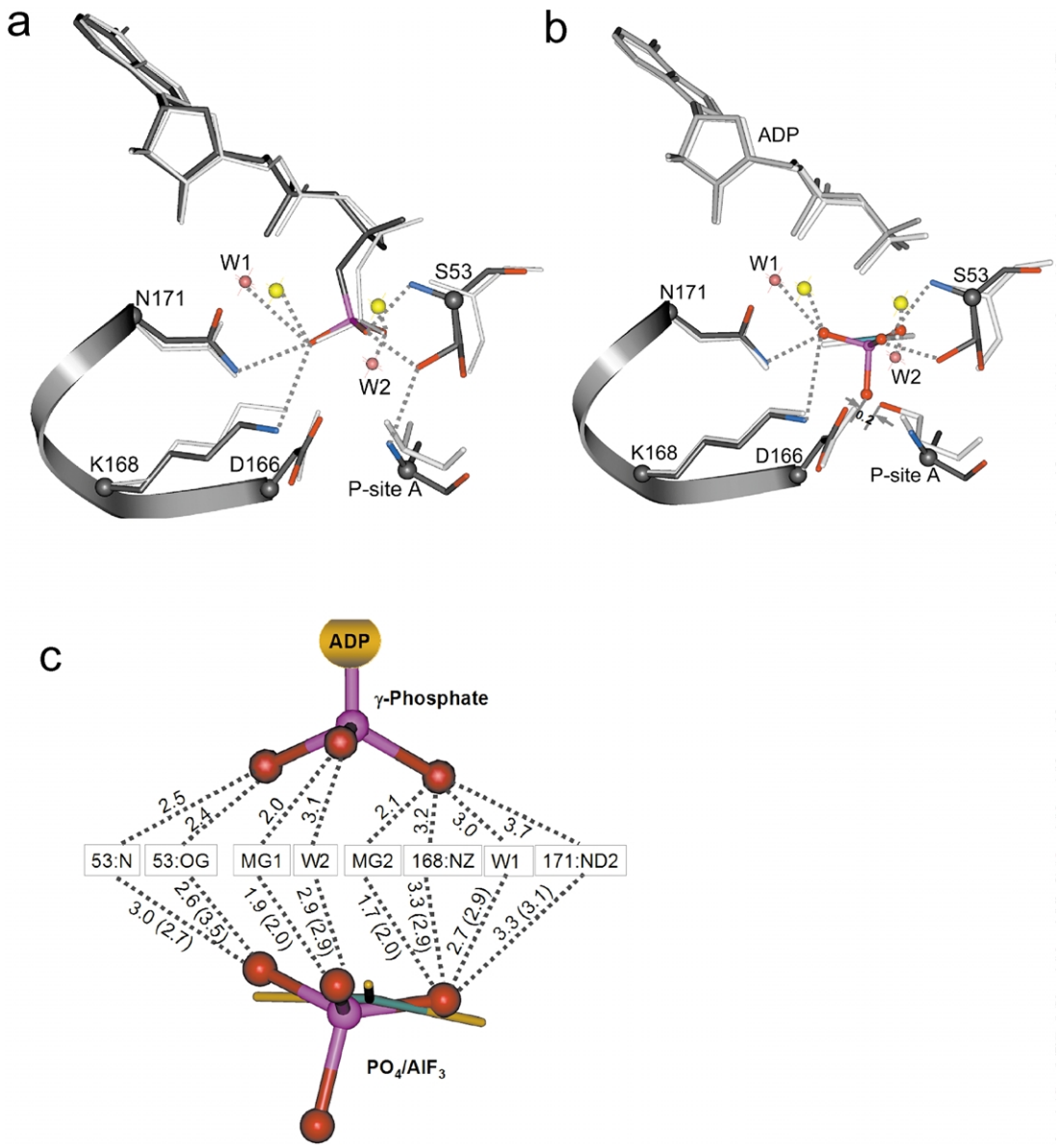

Figure 3. Interaction of nucleotides with active-site residues. a, Superimposition of active sites of the current structure with ATP modeled and that of the wild-type ternary complex (1ATP). Residues from 1ATP are shown in light gray and those from the current structure are shown in gray with oxygen and nitrogen atoms colored in red and blue, respectively. Two magnesium ions are shown as yellow spheres. b, Superimposition of active-site residues of the current structure with ADP-PO_4 and those of the transition state mimic structure (1L3R). The light-gray colored residues are from 1L3R and the rest from the current structure. PO_4 is colored in magenta and red. The aluminum atom is colored in turquoise and fluoride atoms in light gray. c, Comparison of interactions of phosphate/aluminum fluoride with active-site residues. The γ-phosphate group of ATP, PO4 and AlF_3 are shown in real configurations, whereas active-site residues are cartoon-labeled. Dotted lines indicate possible interactions, with distances shown. Interactions with AlF_3 are shown in parentheses.

wild-type was 6.0×10^{-3} unit/mg, and it was fully inhibited by IP20 (Figure 4). In contrast, even though the mutant had similar ATPase activity, it could not be inhibited fully by IP20, even at an IP20/enzyme molar ratio higher (25:1) than that used in the crystallization condition (10:1). Thus it appeared that the hydrolysis of ATP in the Y204A crystal resulted from the uninhibited ATPase activity of the mutant.

Mutation site

The cavity created by the Tyr to Ala mutation was partially filled by two water molecules in the mutant structure (Figure 5a). One (W1) occupied the previous hydroxyl oxygen position, and is within hydrogen bond distance from the side-chain of Glu230, mimicking the interaction between Tyr204 and Glu230 in the wild-type. The

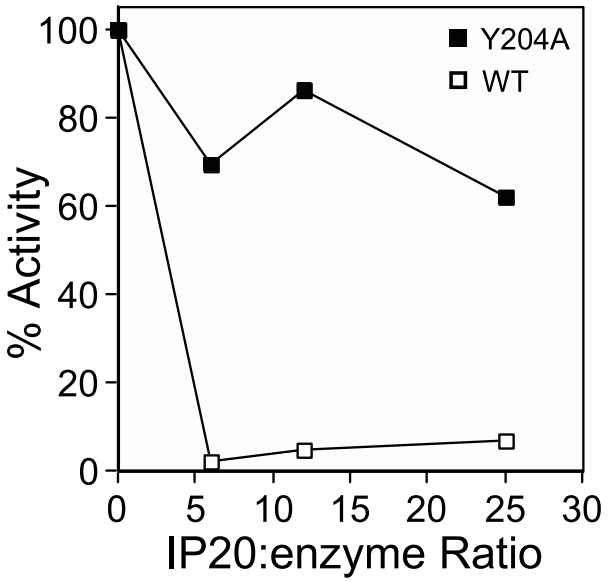

Figure 4. Inhibition of ATPase activity of mutant and wild-type PKAc by IP20. ATPase activity of the wild-type (open square) and the Y204A mutant (closed square) were measured by colorimetric coupled assay. The ATPase activities for the wild-type (6×10^{-3} unit/mg) and mutant (4.0×10^{-3} unit/mg) were taken as 100% separately, to normalize activities measured in the presence of IP20. The amount of IP20 is represented as the molar ratio of IP20 over enzyme.

other water molecule (W2) is within hydrogen bond distance from main-chain atoms from Leu167, Leu227, and Ala223 (Figure 5a). It is interesting to note that the two water molecules were isolated from the solvent environment; the nearest pool of water was more than 5 Å away.

Tyr204 and the hydrophobic core network

Indeed, in the wild-type structure, Tyr204 resides in a highly conserved hydrophobic environment. The unusual hydrophobic αE- and αF-helices constitute the least variable core in the large lobe of the kinase.[10,12] Connecting these two helices is a loop-rich segment (Tyr164–Glu208) that is divided functionally into catalytic loop, Mg-positioning loop, activation loop and P + 1 loop, and contains most of the key residues for enzyme function. The whole segment lies on the top of the core and forms part of the interface between the small and large lobe where the catalysis takes place (Figure 5b). It is held in position mainly through hydrophobic interactions within the segment and with the core. It has been proposed that one function of the hydrophobic core is to serve as a scaffold to hold active-site residues at the surface to carry out catalysis.[12] As illustrated in Figure 5b, residues directly involved in catalysis were positioned to point away from the core toward the active site.[12]

Tyr204 is the only residue coming from the P + 1 loop that participates in the hydrophobic core interactions. Its aromatic ring of Tyr204 interacts mainly with Val226 and Leu227 from the αF-helix, and Pro169 from the catalytic loop (Figure 5c, left). Interactions of these residues with others connect this subsite to the hydrophobic interaction network through the molecule. For example, Leu227 in turn interacts with Leu167, Leu172, Met 231 and other residues, and those that interact with Val226 include Trp222, Pro237 and Leu273. Hydrophobicity of most of these residues is highly conserved throughout the kinase families. According to the kinase sequence database (KSD†), of the 261 aligned animal kinase sequences that did not show a gap at the Tyr204 position, the occurrence of Tyr, Trp and Phe was 61%, 25% and 4%, respectively. In the tyrosine kinases, Trp is seen mostly at the corresponding position. The hydrophobic environment of the Tyr or Trp is structurally conserved, as exemplified by the insulin receptor kinase (Figure 5c, right).[29] The hydroxyl part of Tyr204 is hydrogen bonded with the side-chain of Glu230, the hydrophilic C-terminal end of the αF-helix. Curiously, the corresponding 230 position is always a Glu when it is a Tyr/Trp at the 204 position. Analysis of the available three-dimensional structures indicates that the Tyr/Trp-Glu pairs are likely within hydrogen bond interaction distances, as illustrated in Figure 5(c). These pairs would probably function as a transition from the hydrophobic core to the surface. In the case of PKAc, Glu230 is salt-bridged with Arg133. They seem to create a platform for mediating the interaction with the P-2 Arg residue from the substrate (Figure 5a).

Substrate-induced interaction between Asp166 and Thr201

In an effort to rationalize the effect of the Tyr204 to Ala mutation, we analyzed the detailed interactions for each residue in the P + 1 loop. Thr201 is of particular interest because it is conserved in most kinases and mutation to Ala abolishes PKAc activity. It had been noticed that its side-chain hydroxyl group was in hydrogen bond distance (2.7–3.0 Å) from the carboxylate $O^{\delta 1}$ of Asp166, the invariant catalytic residue in the catalytic loop. To our surprise, by comparing various PKAc structures, we found that this interaction was not present in the structures without substrate or inhibitory peptide bound (Table 2, Figure 6). In the apoenzyme,[12] or when only the nucleotide-binding site was occupied, for example, by adenosine[6] or PKAc inhibitor balanol,[30] the distance between O^{γ} of Thr201 and $O^{\delta 1}$ of Asp166 is greater than 4.5 Å. It seemed that binding of substrate to the P + 1 loop is required to induce this interaction. The other carboxylate oxygen atom, $O^{\delta 2}$, of Asp166 is within hydrogen bond distance from the hydroxyl group of the P-site serine

† http://kinase.ucsf.edu/ksd

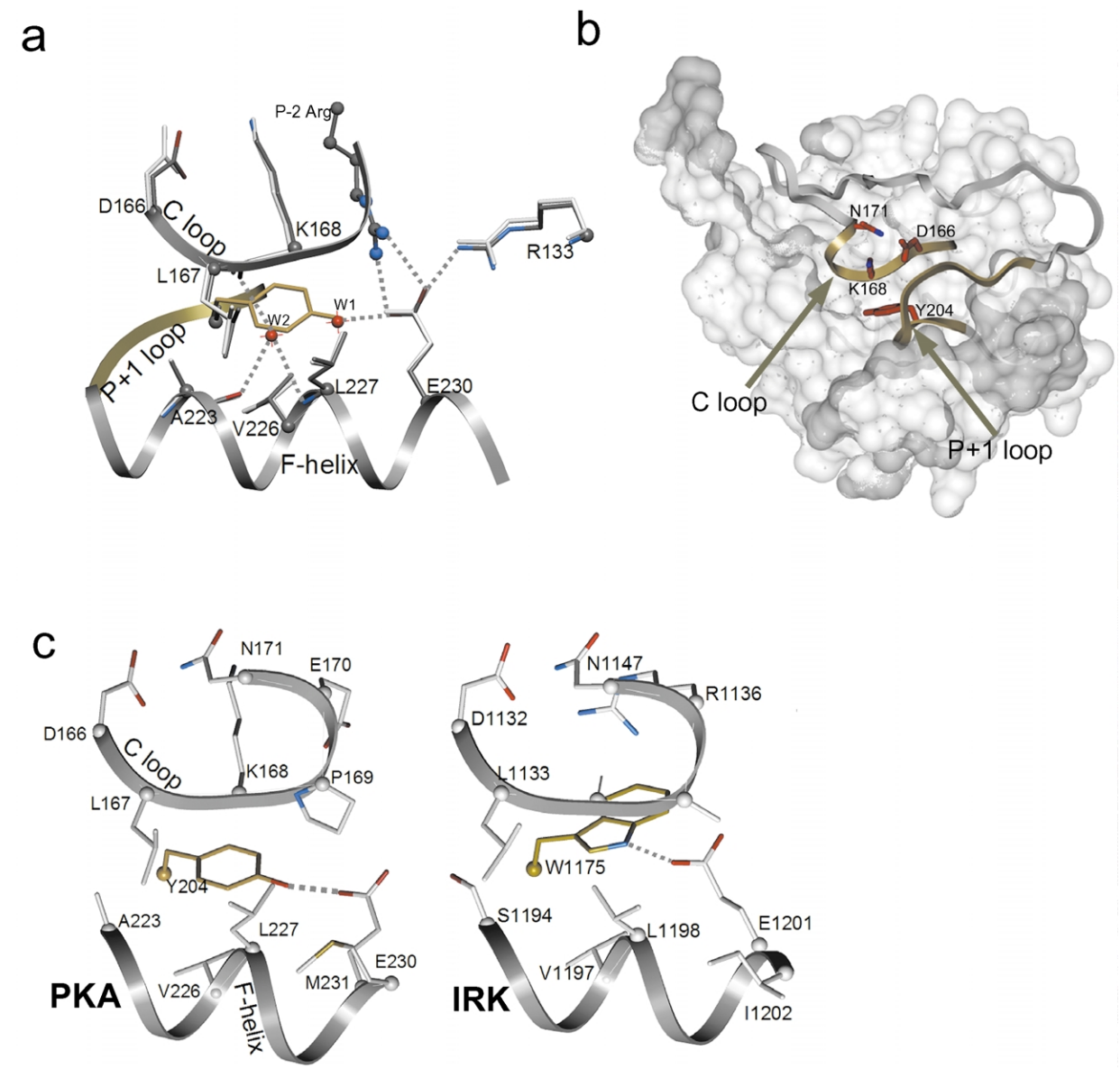

Figure 5. The Tyr204 environment and the hydrophobic core. a, Superimposition of the mutation site of the current structure (gray) with that of 1L3R (light gray, except for Y204, which is colored by tan). Two water molecules in the Y204A structure are shown as red spheres. Dotted lines indicate possible hydrogen bond interactions. The αF-helix and catalytic loop (labeled as C loop) are shown in gray ribbon and part of the P + 1 loop is shown in tan. The P − 2 site Arg is represented with spheres and sticks. b, Anchoring of the catalytically important segment by hydrophobic core. Part of the large lobe (128–164, 209–310) is rendered as partial-transparency solid surface. The segment from 165–208 connecting the αE and αF-helices is rendered as ribbon, with the catalytic loop and P + 1 loop colored in tan. Catalytic residues Asp166, Lys168 and Asn171 pointing out toward the active site, and Tyr204, interacting with the core, are highlighted as red sticks. c, Conservation of the hydrophobic core. PKAc (represented by 1L3R, left) was superimposed with the insulin receptor kinase domain (PDB ID 1IR3, right) and then separated transitionally for better visualization.

residue, or in the current structure, PO4:O4, the oxygen atom coming from the attacking water molecule. In some of the structures, $O^{\delta 2}$ of Asp166 might form a weaker hydrogen-bond interaction with $N^{\delta 2}$ of Asn171 (3.0–3.4 Å); the interaction had no correlation with nucleotide or peptide substrates. It is thus possible that upon binding of substrate, Asp166 is further stabilized by interacting with Thr201 in the conformation that in turn can align the P-site hydroxyl group for in-line attack of the γ-phosphorus group.

The importance of Thr201 is further demonstrated by its interaction with the side-chain of Lys168 (Table 2, Figure 6), another critical residue in the catalytic loop, where mutation to Ala or Met caused loss of activity[31] (M. Valiev, J.Y., M. Deal, J. Penny & S.T., unpublished results). However, this interaction is not correlated with the binding of substrates.

Table 2. Interaction between Thr201 and Asp166 upon substrate binding

PDB ID of PKA structure	Ligand	O^{γ} (T201) to $O^{\delta 1}$ (D166) (Å)	O^{γ} (T201) to $N^{\zeta 1}$ (K168) (Å)
1J3H	Unliganded	5.0	3.3
1BKX	Adenosine	4.5	4.0
1BX6	Balanol	4.9	3.4
1JLU	SP20	3.1	3.0
2CPK	IP20	2.9	2.8
1YDT	H89[a]/IP20	3.1	3.0
1CDK	MnAMPPNP/IP20	2.7	2.9
1L3R	MgADP/AIF/SP20	2.8	2.9
1ATP	MnATP/IP20	2.8	3.0
Y204A[b]	MgATP/IP20	2.8	2.8

[a] H89, *N*-[2-(4-bromocinnamylamino)ethyl]-5-isoquinoline.
[b] Current data, PDB ID 1RDQ.

Discussion

"*In situ*" ATP hydrolysis in the Y204A crystal

The function of protein kinases is to transfer the γ-phosphate group from ATP to another protein molecule. Some kinases, including PKAc, also exhibit ATPase activity that is energetically wasteful and so is greatly suppressed by structurally excluding the free water molecule from the active site. The nucleotide-binding site is much more solvent-accessible in proteins that function as ATPases or GTPases where, often, the phosphoacceptor water molecule could be trapped in the crystal structures with a non-hydrolyzabe nucleotide analog.[32,33] Protein kinases, however, are structured to efficiently exclude free water from their active site. It has been shown that the high-affinity binding of IP20 to PKAc excludes water from the active site very efficiently and results in full inhibition of its ATPase activity.[28] It is thus surprising that in the current structure, we observed hydrolysis of ATP in the crystals of Y204A with IP20 bound. In light of the experimental data showing that IP20 could not fully abolish the ATPase activity of the mutant (Figure 4), we argue that the observation is not because of high resolution but rather the dynamic property of the mutant (see below): somehow, water can still diffuse slowly into the active site even in the presence of IP20.

The retention of the hydrolyzed products ADP-PO_4 is another surprise, since, generally, small molecules as such could diffuse into the solvent easily. Summarizing earlier kinetic and structural analysis on PKAc, we know that the cooperative binding of nucleotide and peptide substrates and the sequential release of the phosphorylated peptide and ADP, are enabled structurally by the opening and closure of the active-site cleft.[34–36] The retention of ADP-PO_4 is in agreement with this concept: the binding of IP20 causes the active site to remain closed even after phosphoryl transfer has been completed so that the reaction products are trapped.

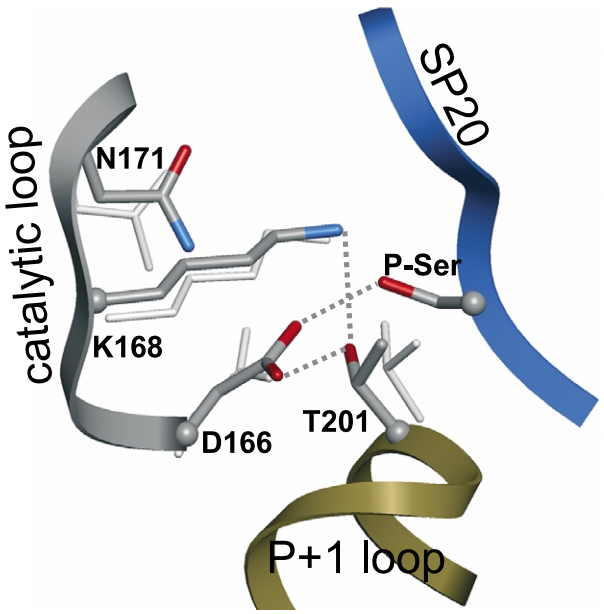

Figure 6. Substrate-induced interaction between Asp166 and Thr201. The structure of apo-PKAc (1J3H) was superimposed with the ternary structure, represented by 1L3R. Residues from 1J3H structure are shown in light gray and those from 1L3R are shown in gray with side-chain oxygen (red) and nitrogen (blue) colored. Catalytic loop, P + 1 loop and substrate part of the substrate peptide were shown as ribbons. C^{α} atoms were rendered as spheres. Dotted lines indicate possible interactions in the ternary complex. Distances are shown in Table 2.

Insight into the catalytic mechanism

We have already solved several binary or ternary PKAc structures complexed with either nucleoside/nucleotide or peptide or both, which, to some extent, represent snapshots of the active site at different stages along the catalytic pathway. The coexistence of the two nucleotide states in the same crystal allows, in a more "real" setting, a better comparison of the active site prior to and immediately after phosphoryl transfer. The facts that active-site residues take single conformations and that the ADP moiety of ATP is in a position nearly identical with that of the product ADP, suggest strongly that during the phosphoryl transfer, the active site conformation remains unchanged except for the "travel" of the γ-phosphorus atom toward the attacking water molecule to generate the free phosphate group. This is consistent with the earlier speculation, that the ternary complex of PKA complexed with Mg·ATP and the inhibitory peptide actually assumed a "transition state-like" conformation with the γ-phosphate group poised for transfer but having no acceptor available.[8,23] The current Y204A ternary structure is virtually in such a state, except now a water molecule could apparently diffuse slowly into the

active site. With every residue in the "ready" conformation for phosphoryl transfer, once the water molecule diffuses in, it gets positioned by Asp166 (see below) and the reaction proceeds immediately.

The significance of the possible strong interaction of the P-site amide group with the Ser53 side-chain in the B-conformation (2.6 Å) (Figure 2c) is not clear. It may further secure the glycine-rich loop and the substrate toward the active site in a concerted manner during the phosphoryl transfer process. A similar interaction (3.2 Å) was seen in the aluminum fluoride transition state mimic structure (1L3R). However, in the ternary PKAc:Mn·ATP:IP20 (1ATP) and PKAc:Mn·AMPPNP:IP20 (1CDK), the distance was 3.6–3.8 Å, and the active site was fully closed. The distance was greater than 5 Å with an intermediate or open active site conformation, due to the glycine-rich loop moving away from the large lobe. All these observations suggest that the Ser53 side-chain may adopt conformation B during phosphoryl transfer.

Questions have been raised as to which of the residues that interact with ATP "follows" the reaction to the transition state.[38] Comparing the interaction of active-site residues with the γ-phosphate group of ATP, AlF_3 and the product PO_4, we see that most of the residues keep the same interactions as phosphoryl transfer proceeds (Figure 3). These include the two metal ions, two structured water molecules, the Ser53 amide group and the Lys168 side-chain. In light of a contracted active site and the "rigidity" of the active-site conformation during the phosphoryl transfer, we speculate that these residues may be utilized to stabilize the transition state. A role for Lys168 in stabilizing the transition state has been proposed, based on its conservation and its effect on the kinetics.[7,23] Since interaction of the Ser53 amide group with PO_4 appears somewhat weaker than with the γ-phosphate group, it is possible that the Ser53 side-chain may assume conformation B in the transition state to further strengthen the interaction with the phosphate. It is intriguing though, that previous kinetic analysis showed no changes in the phosphoryl transfer rate on the Ser53Ala mutant.[37] If this side-chain does play a role, it would appear to not be rate-limiting.

Anchoring of the P + 1 loop to the hydrophobic core and its connection to the catalytic loop

Akamine *et al.*[12] have recently proposed a role for the hydrophobic core as a platform for anchoring catalytic residues. In analyzing the structure and function of the P + 1 loop and Tyr204, we are able to appreciate better how this loop is anchored through the hydrophobic interaction of Tyr204 with the core. Here, we expand this concept to a more "global" view that, as a very stable and conserved substructure, this core might serve to anchor other functional loops/residues in different parts of the molecule and thereby mediate long-distance communication between them. In the P + 1 loop, Leu198–Leu205, only Tyr204 makes contact with the kinase core; the other residues participate mainly in substrate binding. Further down, Glu208 forms a conserved ion pair with Arg280, which in turn packs against Trp222 from the αF-helix, a signal integration motif that is linked to the catalytic loop through interaction of Asp220 with Tyr164 and Arg165. The concerted action of this helix may thus serve to anchor and stabilize both the catalytic loop and the P + 1 loop region (Figure 7). Database analysis indicates that the hydrophobicity of Tyr204 is highly conserved, and its interaction with the hydrophobic core is likely to be structurally conserved as well (Figure 3). In agreement, experimental data show that the Y204A mutant exhibits significantly altered kinetic properties[15] and reduced thermostability (J.Y., J. Canaves & S.T., unpublished results).

The P + 1 loop is part of the activation segment defined between the two conserved motifs ^{184}DFG and APE^{208}. In the inactive form of the kinase, this segment assumes a very dynamic conformation pointing toward the active site but is flipped nearly 180° outward to the edge in the active form. The two hinge points are residue Asp1150 and Pro1172 in the insulin receptor kinase (IRK),[39,40] and Asp145 and Leu166 in the cyclin-dependent protein kinase (CDK2),[41,42] which correspond to Asp184 and Pro202 in PKAc. Thus, in a more global context, interaction of Tyr204 or the corresponding residues in other kinases with the hydrophobic core serves as an anchoring point for the activation segment.

The essential role of Asp166 in catalysis has been well established, even though it is not clear whether it acts as a catalytic base to extract a proton from the hydroxyl moiety of phosphoacceptor or to simply align it for nucleophilic attack.[43] Very recently, based on first principle quantum mechanical calculations, Marat *et al.* have proposed that Asp166 most likely function as a "proton trap" to accept the proton from the phosphoacceptor hydroxyl group after phosphoryl transfer.[44] Comparing the available PKAc structures with different ligands/substrates, we find that the interaction between $O^{\delta 1}$ of Asp166 and O^{γ} of Thr201 is present only when peptide inhibitor/substrate is present. The other carboxylate oxygen atom of Asp166 is within hydrogen bond distance of the hydroxyl group from the phosphoacceptor (a water molecule in the current structure, Figure 7). We speculate that this substrate-induced interaction between Thr201 and Asp166 helps to lock Asp166 in the conformation that is necessary for interacting with the phosphoacceptor hydroxyl group. This may be an important preparation for catalysis. Thr201 is highly conserved among Ser/Thr kinases and the mutation to Ala in PKAc abolished enzyme activity.

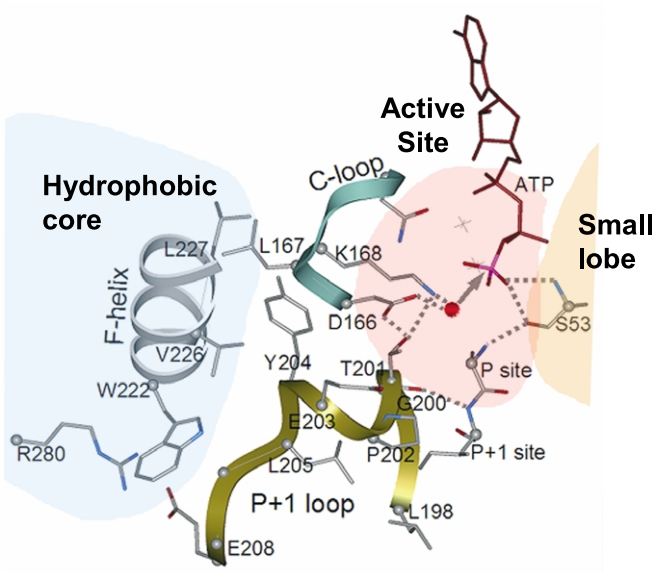

Figure 7. Function of the P + 1 loop, which is anchored to the hydrophobic core through interaction with the αF-helix. Interaction among Tyr204, Val226, Leu227 and Leu167 forms the major anchoring site, which is probably augmented by the hydrophobic packing of Glu208:Arg280 ion pair with Try222. Residues from the P + 1 loop provide multiple interactions with the substrate: Leu198, Pro202 and Leu205 form the binding pocket for the side-chain of the P + 1 residue, whereas the carbonyl group of Gly200 interacts with its amide group. Interaction of Glu203 with P − 2 Arg is not shown. Binding of substrate/IP20 to the P + 1 loop induces the interaction between Thr201 and Asp166, so the water molecule (shown in red sphere) that diffuses into the active site is aligned for nucleophilic attack (cartooned as a gray arrow) of the γ-phosphorus atom of ATP to form ADP-PO_4. The hydrophobic core, small lobe and active site are shaded in light blue, orange and pink, respectively.

In most Ser/Thr kinases, the residue immediately preceding Thr201 is Gly.[13,45] In the CMGC subfamily, however, non-glycine residues are usually seen. In such kinases, when the activation segment adopts the active conformation, the non-Gly residue assumes unfavorable backbone ϕ−ψ angles. This restrained conformation seems to associate only with the active conformation of the activation segment. Mutation of Gly200 to Ala in PKAc,[15] or mutation of the non-Gly residue to Gly in a CMGC family kinase Sky1p[46] both resulted in loss of enzyme activity, suggesting that the residue at this position is critical for responding to conformational changes of the activation segment during catalysis.

In summary, Tyr204 serves to anchor the P + 1 loop to the hydrophobic core through packing with Val226 and Leu227 from the αF-helix. The anchoring is probably augmented by the Glu208:Arg280 pair packing against Trp222 at the other end of the same helix (Figure 7). These hydrophobic anchors appear to be conserved in most protein kinases and can be viewed as anchoring points for the activation segment. The conformation of the P + 1 loop appears to be important for kinase activity and substrate recognition. Residues from the loop participate in direct contact with the substrate, they are also directly (Thr201−Asp166) or indirectly (Tyr204-αF-helix-Leu167, Tyr164, Arg165) associated with the catalytic loop, so that the catalytic residues can sense the presence of the substrate (Figure 7). This is consistent with the dramatic alteration in k_{cat} that is seen for the Y204A mutant. Akamine *et al.* have proposed that the hydrophobic core may mediate communication between the nucleotide and peptide substrates. Here, we see another example of it mediating communication between substrate binding and phosphoryl transfer.

Dynamic effect of Tyr204 to Ala mutation

Even though the Y204A mutant exhibited a dramatic difference in kinetic properties from the wild-type enzyme, and even though IP20 could fully inhibit the ATPase activity of wild-type but not that of the mutant enzyme, the crystal structure of the mutant PKAc was very similar to that of the wild-type. From the structural analysis, it is likely that the mutation may disrupt the anchoring of the P + 1 loop and thereby overall peptide binding as well as catalysis. It may also destabilize the hydrophobic core. In addition, it could alter the communication between the P + 1 loop and the catalytic loop. All these effects are at the dynamic level, and may not be reflected in the crystal structure. The mutation could provide the enzyme molecule with a more flexible P + 1 loop that would influence its initial association with the substrate/inhibitor peptide. The efficiency of excluding water from the active site would be reduced, so that a water molecule could diffuse in slowly to participate in the hydrolysis of ATP. Once the substrate is bound to the enzyme, the interactions between the two, which are as observed in the crystal structure, would exhibit no difference from those seen in the wild-type enzyme. The dynamic destabilization of the P + 1 loop could affect the dynamic interaction between Thr201 and Asp166, and these could affect the alignment of the nucleophilic hydroxyl group from the substrate. These could account for the altered K_m and k_{cat}. The bound IP20 in the crystal

structure most likely accounts for the failure to observe a more flexible P + 1 loop, since its binding would force the loop into the conformation that prepares the catalytic-site residues for catalysis. Utilizing hydrogen/deuterium exchange coupled with mass spectrometry, we found that the catalytic loop in the Tyr204 mutant protein showed decreased amide hydrogen protection, which is consistent with increased dynamics in the localized region (J.Y., S. Garrod, C. Juliano, M. Deal & S.T., unpublished results). This is strong evidence for the dynamic effect of the mutant, and it shows that this effect can transmit from the P + 1 loop to the catalytic loop. It is reasonable to speculate that the increased dynamics in the catalytic loop would affect the kinetics of the mutant.

Through the above analysis of the phosphoryl transfer at the active site and trying to understand the role of Tyr204, we can appreciate the beauty of the kinase architecture for orchestrating the transfer of phosphate to protein substrate. The helix-dominant large lobe provides a pre-formed docking site for substrate and a stable platform to anchor and stabilize important loop segments and residues therein. It might serve also as a communication center to integrate and transmit information from different parts of the molecule. In contrast, the flexibility of the small lobe allows it to move relative to the position of the large lobe, so the enzyme can adopt an ensemble of open and closed active-site conformations, which is an essential structural basis for the catalytic cycle. Cooperative binding of nucleotide and peptide substrates "closes up" the active site and positions the catalytic residues for phosphoryl transfer. The active site remains in a similar conformation during the process to keep the reaction barrier low and the phosphoryl transfer rate high. We appreciate more fully the importance of integrating dynamic and static information in order to understand better enzyme function. In this particular case, due to the dynamic effect caused by the Tyr204 to Ala mutation, we were able to capture the active site in pre- and post-phosphotransfer conformations. Putting together all the information we gained from this structure and others, we can literally "visualize" the phosphoryl transfer process. Cooperative binding of nucleotide and peptide substrates engages the enzyme in a "transition state-like" conformation with the γ-phosphate group poised for transfer. This includes the stabilization of the Asp166 conformation through its interaction with Thr201 in a substrate-dependent manner (Figure 6), so that when a substrate or, in this case, water molecule diffuses in, it is positioned by Asp166 for in-line attack of the γ-phosphorus atom and the phosphoryl transfer takes place immediately (Figure 7). Even though here we have captured the transfer of phosphate to a water molecule, we believe this same mechanism should apply for transferring phosphate to a protein acceptor.

Materials and Methods

Materials

Inhibitory peptide IP20 (TTYADFIASGRTGRRN AIHD), residues 5–24 from the heat-stable PKAc inhibitor PKI, was synthesized on a Milligen peptide synthesizer and purified by high-performance liquid chromatography. The prepacked MonoS 10/10 ion-exchange column and Superdex 75 preparation grade resin were from Amersham Biosciences. Precast Nu-PAGE and isoelectric-focusing gels were purchased from Invitrogen. Crystallization reagents MPD, glycerol, bicine (*N*,*N*-bis-(2-hydroxyethyl)-glycine) and ammonium acetate were from Fluka. Other reagents were from Invitrogen, Roche Applied Science and Sigma-Aldrich.

Protein purification and crystallization

Tyr204 to Ala mutation in the murine PKA catalytic subunit C^{α} was introduced as reported.[15] Although the Y204A mutant exhibited significantly decreased catalytic efficiency, it adopted the active conformation when expressed in *Escherichia coli*, as did the wild-type enzyme.[47] The purification procedure was similar to that used for the wild-type protein.[48] Major changes included using phosphate buffer at pH 7.0 instead of pH 6.5 in the MonoS chromatography, since this was necessary and efficient for separating the mutant protein from an *E. coli* contaminant. For crystallization samples, an additional chromatography on a Superdex 75 column (12 cm × 60 cm) was introduced. Protein was eluted with 50 mM bicine, 200 mM ammonium acetate (pH 8.0) plus 2 mM dithothreitol, and concentrated to 5 mg/ml. Y204A crystals were grown in the presence of $MgCl_2$, ATP and IP20. The protein (80 μM) was pre-mixed with $MgCl_2$, ATP and IP20 at a molar ratio of 1:10:10:10. The drop consisted of 2 μl of this protein mixture and 1 μl of well solution containing 8–12% (v/v) MPD plus 10 mM DTT. Methanol (7–10% (v/v) was added to the well before sealing the cover-slip.[49]

Data collection

Although the crystal of Y204A was quite small, it diffracted beyond 1.2 Å under the synchrotron source. A 1.26 Å resolution data set was collected on beamline 7.1 at Stanford Synchrotron Radiation Laboratory (Menlo Park, CA), using two passes. An initial pass collected data to 1.45 Å, the later one collected data from 1.26–2 Å. All data collection was performed at 100–110 K. The cryoprotectant consisted of 15% (v/v) MPD, 15% (v/v) glycerol and 50 mM bicine (pH 8.0). The two data sets were processed and scaled separately with DENZO/SCALEPACK and then scaled into one set.[50] The statistics are shown in Table 1. Although the Y204A mutant crystallized in the same $P2_12_12_1$ space group as most of the wild-type protein crystals,[21] its cell dimensions were different. Most of the wild-type crystals, irrespective of what they were co-crystallized with, had very similar cell dimensions, with $a = 73.58$ Å, $b = 76.28$ Å, $c = 80.58$ Å, as in the ternary complex PKAc:Mg·ATP:IP20 (1ATP).[8] The Y204A crystal, however, has cell dimensions of $a = 57.76$ Å, $b = 79.51$ Å, $c = 97.74$ Å.

Refinement of the model

The initial structure of Y204A was solved by molecular replacement using Crystallography and NMR System (CNS).[51] The binary structure PKAc:IP20 (PDB ID 1APM) was used as the starting model. With 5% of the data kept as a reference set for calculating cross-validation R_{free}, this model was refined against the 1.26 Å data set using CNS to R of 20.0%, and R_{free} of 20.8%, with 300 water molecules included. The refinement was then continued with SHELXL 97[52] to carry out the anisotropic displacement parameter refinement to further improve the model. Since this 1.26 Å data set is in the gray zone for anisotropic displacement parameter refinement due to its resolution and its incompleteness in the highest-resolution shell, different restraints were tested using R_{free} as a monitor. While rigid body restraint for anisotropic displacement parameter (term DEFS) was kept at the default value of 0.02, the similarity restraint (term SIMU) was set to 0.1, 0.08 or 0.05. Tightening the SIMU restraint from 0.1 to 0.05 improved the R_{free} by 0.2%, and was thus used throughout the anisotropic displacement parameter refinement. Introducing individual anisotropic displacement parameter resulted in a decrease of 2.4% in R and 1.6% in R_{free}, validating the refinement. Riding hydrogen atoms were introduced in the last runs of refinement, and they led to a decrease of 0.8% in both R and R_{free}.

The final model was refined to R of 13.2% and R_{free}, of 16.3%. As assessed by PROCHECK,[52] 91.3% of the main-chain ϕ/ψ torsion angles were in the core region in the Ramachandran plot, and the remaining 8.7% were in the allowed region. A noticeable deviation is the main-chain planarity of Val123. The ω value is 202°, which is highly different from the statistical value. It is worth mentioning this, because this residue is involved in the interaction with the adenine ring of the ATP molecule. Although the discrepancy in the peptidyl bond planarity is not uncommon in the atomic structure refinement,[53] this high degree of deviation is still striking. In the refinement of the 1.25 Å structure of cholera toxin B-pentamer, it was found that in the region of the receptor-binding site, one of the peptide groups was highly non-planar, with ω value of 154°.[54] Analysis of anisotropic displacement parameters by the Protein Anisotropic Refinement and Validation Tool†[55] showed an average anisotropy of 0.422 ± 0.145, 0.393 ± 0.143, and 0.497 ± 0.176 for protein atoms, oxygen atoms from water molecules, and heteroatoms, respectively, in good agreement with the statistics obtained by analyzing over 60 other structures with the available anisotropic displacement parameters.[55]

Modeling of nucleotide

During high-resolution refinement with SHELXL, when ATP was modeled at the nucleotide-binding pocket, the bond length between the β-γ bridge oxygen atom (O3B) and the γ-phosphorus atom (P3) was refined persistently to greater than 1.9 Å, significantly longer than the targeted value of 1.65 Å. Negative electron density was observed along the bond. Omit maps indicated the possibility of mixed occupancies of ATP and its hydrolyzed product ADP-PO_4. Occupancy refinement using different starting values (0.1–0.9 for ATP, interval of 0.1) strongly suggested a convergence at 0.26 occupancy for ATP and 0.74 for ADP-PO_4.

Kinase activity and ATPase activity assays

Specific activities of wild-type and mutant enzymes were determined using kemptide (LRRASLG) as substrate, by the coupled assay described by Cook *et al.*[56] ATPase activity was measured by the same method, except in the absence of substrate peptide and using much larger amounts of enzymes. Typically, the ATPase activity assay was measured by incubating 15 μM enzyme with 1 mM ATP in the presence or in the absence of 10–400 μM IP20.

Protein Data Bank accession code

The coordinates and reflection data have been deposited in to the RCSB Protein Data Bank. The PDB ID for the Y204A structure with partial ATP and ADP-PO_4 is 1RDQ.

† http://www.bmsc.washington.edu/parvati/parvati.html

Acknowledgements

We thank Jian Wu, Pearl Akamine, Madhusudan, Debing Huang (Department of Chemistry, University of California San Diego), Chris Waddling (Macromolecular structure group, University of California San Francisco) & Xueyong Zhu (The Scripps Research Institute) for their valuable help in structure determination and refinement; Ganesh Anand, Ganesh Iyer & Joseph Adams (Department of Pharmacology, University of California San Diego) for inspiring discussions, and Elzbieta Radzio-Andzelm for help with Figures. We thank the scientists at beamline 7.1 at Stanford Synchrotron Radiation Laboratory (Menlo Park, CA) for data collection assistance. Parts of the computational and graphic work were performed at the W. M. Keck Laboratory for Integrated Biology II (La Jolla, CA). This work is supported by grant GM19301 to S. S. T.

References

1. Taylor, S. S., Radzio-Andzelm, E. & Hunter, T. (1995). How do protein kinases discriminate between serine/threonine and tyrosine? Structural insights from the insulin receptor protein-tyrosine kinase. *FASEB J.* **9**, 1255–1266.
2. Taylor, S. S. & Radzio-Andzelm, E. (1994). Three protein kinase structures define a common motif. *Structure*, **2**, 345–355.
3. Taylor, S. S., Knighton, D. R., Zheng, J., Sowadski, J. M., Gibbs, C. S. & Zoller, M. J. (1993). A template for the protein kinase family. *Trends Biochem. Sci.* **18**, 84–89.
4. Johnson, D. A., Akamine, P., Radzio-Andzelm, E., Madhusudan, M. & Taylor, S. S. (2001). Dynamics of cAMP-dependent protein kinase. *Chem. Rev.* **101**, 2243–2270.
5. Madhusudan, M., Akamine, P., Xuong, N. H. &

Taylor, S. S. (2002). Crystal structure of a transition state mimic of the catalytic subunit of cAMP-dependent protein kinase. *Nature Struct. Biol.* **9**, 273–277.
6. Narayana, N., Cox, S., Nguyen-huu, X., Ten Eyck, L. F. & Taylor, S. S. (1997). A binary complex of the catalytic subunit of cAMP-dependent protein kinase and adenosine further defines conformational flexibility. *Structure*, **5**, 921–935.
7. Madhusudan, M., Trafny, E. A., Xuong, N. H., Adams, J. A., Ten Eyck, L. F., Taylor, S. & Sowadski, J. M. (1994). cAMP-dependent protein kinase: crystallographic insights into substrate recognition and phosphotransfer. *Protein Sci.* **3**, 176–187.
8. Zheng, J., Knighton, D. R., ten Eyck, L. F., Karlsson, R., Xuong, N., Taylor, S. S. & Sowadski, J. M. (1993). Crystal structure of the catalytic subunit of cAMP-dependent protein kinase complexed with MgATP and peptide inhibitor. *Biochemistry*, **32**, 2154–2161.
9. Knighton, D. R., Zheng, J. H., Ten Eyck, L. F., Xuong, N. H., Taylor, S. S. & Sowadski, J. M. (1991). Structure of a peptide inhibitor bound to the catalytic subunit of cyclic adenosine monophosphate-dependent protein kinase. *Science*, **253**, 414–420.
10. Knighton, D. R., Zheng, J. H., Ten Eyck, L. F., Ashford, V. A., Xuong, N. H., Taylor, S. S. & Sowadski, J. M. (1991). Crystal structure of the catalytic subunit of cyclic adenosine monophosphate-dependent protein kinase. *Science*, **253**, 407–414.
11. Murzin, A. G., Brenner, S. E., Hubbard, T. & Chothia, C. (1995). SCOP: a structural classification of proteins database for the investigation of sequences and structures. *J. Mol. Biol.* **247**, 536–540.
12. Akamine, P., Madhusudan, M., Wu, J., Xuong, N. H., Ten Eyck, L. F. & Taylor, S. S. (2003). Dynamic features of cAMP-dependent protein kinase revealed by apoenzyme crystal structure. *J. Mol. Biol.* **327**, 159–171.
13. Hanks, S. K. & Quinn, A. M. (1991). Protein kinase catalytic domain sequence database: identification of conserved features of primary structure and classification of family members. *Methods Enzymol.* **200**, 38–62.
14. Johnson, L. N. (2001). Structural basis for substrate recognition and control in protein kinases. *Ernst Schering Res. Found Workshop*, 47–69.
15. Moore, M. J., Adams, J. A. & Taylor, S. S. (2003). Structural basis for peptide binding in protein kinase A. Role of glutamic acid 203 and tyrosine 204 in the peptide-positioning loop. *J. Biol. Chem.* **278**, 10613–10618.
16. Grant, B. D. & Adams, J. A. (1996). Pre-steady-state kinetic analysis of cAMP-dependent protein kinase using rapid quench flow techniques. *Biochemistry*, **35**, 2022–2029.
17. Hemmer, W., McGlone, M., Tsigelny, I. & Taylor, S. S. (1997). Role of the glycine triad in the ATP-binding site of cAMP-dependent protein kinase. *J. Biol. Chem.* **272**, 16946–16954.
18. Suel, G. M., Lockless, S. W., Wall, M. A. & Ranganathan, R. (2003). Evolutionarily conserved networks of residues mediate allosteric communication in proteins. *Nature Struct. Biol.* **10**, 59–69.
19. Lockless, S. W. & Ranganathan, R. (1999). Evolutionarily conserved pathways of energetic connectivity in protein families. *Science*, **286**, 295–299.
20. Smith, C. M., Radzio-Andzelm, E., Madhusudan, M., Akamine, P. & Taylor, S. S. (1999). The catalytic subunit of cAMP-dependent protein kinase: prototype for an extended network of communication. *Prog. Biophys. Mol. Biol.* **71**, 313–341.
21. Narayana, N., Cox, S., Shaltiel, S., Taylor, S. S. & Xuong, N. (1997). Crystal structure of a polyhistidine-tagged recombinant catalytic subunit of cAMP-dependent protein kinase complexed with the peptide inhibitor PKI(5-24) and adenosine. *Biochemistry*, **36**, 4438–4448.
22. Zheng, J., Knighton, D. R., Xuong, N. H., Taylor, S. S., Sowadski, J. M. & Ten Eyck, L. F. (1993). Crystal structures of the myristylated catalytic subunit of cAMP-dependent protein kinase reveal open and closed conformations. *Protein Sci.* **2**, 1559–1573.
23. Bossemeyer, D., Engh, R. A., Kinzel, V., Ponstingl, H. & Huber, R. (1993). Phosphotransferase and substrate binding mechanism of the cAMP-dependent protein kinase catalytic subunit from porcine heart as deduced from the 2.0 Å structure of the complex with Mn2 + adenylyl imidodiphosphate and inhibitor peptide PKI(5-24). *EMBO J.* **12**, 849–859.
24. Yang, J., Cron, P., Thompson, V., Good, V. M., Hess, D., Hemmings, B. A. & Barford, D. (2002). Molecular mechanism for the regulation of protein kinase B/Akt by hydrophobic motif phosphorylation. *Mol. Cell*, **9**, 1227–1240.
25. Yang, J., Cron, P., Good, V. M., Thompson, V., Hemmings, B. A. & Barford, D. (2002). Crystal structure of an activated Akt/protein kinase B ternary complex with GSK3-peptide and AMP-PNP. *Nature Struct. Biol.* **9**, 940–944.
26. Biondi, R. M., Komander, D., Thomas, C. C., Lizcano, J. M., Deak, M., Alessi, D. R. & van Aalten, D. M. (2002). High resolution crystal structure of the human PDK1 catalytic domain defines the regulatory phosphopeptide docking site. *EMBO J.* **21**, 4219–4228.
27. Goldsmith, E. J. & Chang, C. I. (2002). Another twist in helix C and a missing pocket. *Structure (Camb.)*, **10**, 888–889.
28. Mendelow, M., Prorok, M., Salerno, A. & Lawrence, D. S. (1993). ATPase-promoting dead end inhibitors of the cAMP-dependent protein kinase. *J. Biol. Chem.* **268**, 12289–12296.
29. Hubbard, S. R. (1997). Crystal structure of the activated insulin receptor tyrosine kinase in complex with peptide substrate and ATP analog. *EMBO J.* **16**, 5573–5581.
30. Narayana, N., Diller, T. C., Koide, K., Bunnage, M. E., Nicolaou, K. C., Brunton, L. L. *et al.* (1999). Crystal structure of the potent natural product inhibitor balanol in complex with the catalytic subunit of cAMP-dependent protein kinase. *Biochemistry*, **38**, 2367–2376.
31. Gibbs, C. S. & Zoller, M. J. (1991). Rational scanning mutagenesis of a protein kinase identifies functional regions involved in catalysis and substrate interactions. *J. Biol. Chem.* **266**, 8923–8931.
32. Ihara, K., Muraguchi, S., Kato, M., Shimizu, T., Shirakawa, M., Kuroda, S. *et al.* (1998). Crystal structure of human RhoA in a dominantly active form complexed with a GTP analogue. *J. Biol. Chem.* **273**, 9656–9666.
33. Braig, K., Menz, R. I., Montgomery, M. G., Leslie, A. G. & Walker, J. E. (2000). Structure of bovine mitochondrial F(1)-ATPase inhibited by Mg(2 +) ADP and aluminium fluoride. *Struct. Fold. Des.* **8**, 567–573.
34. Li, F., Gangal, M., Juliano, C., Gorfain, E., Taylor, S. S. & Johnson, D. A. (2002). Evidence for an internal entropy contribution to phosphoryl transfer: a study

of domain closure, backbone flexibility, and the catalytic cycle of cAMP-dependent protein kinase. *J. Mol. Biol.* **315**, 459–469.
35. Zhou, J. & Adams, J. A. (1997). Participation of ADP dissociation in the rate-determining step in cAMP-dependent protein kinase. *Biochemistry,* **36**, 15733–15738.
36. Adams, J. A. & Taylor, S. S. (1993). Divalent metal ions influence catalysis and active-site accessibility in the cAMP-dependent protein kinase. *Protein Sci.* **2**, 2177–2186.
37. Aimes, R. T., Hemmer, W. & Taylor, S. S. (2000). Serine-53 at the tip of the glycine-rich loop of cAMP-dependent protein kinase: role in catalysis, P-site specificity, and interaction with inhibitors. *Biochemistry*, **39**, 8325–8332.
38. Matte, A., Tari, L. W. & Delbaere, L. T. (1998). How do kinases transfer phosphoryl groups? *Structure*, **6**, 413–419.
39. Hubbard, S. R. (1997). Crystal structure of the activated insulin receptor tyrosine kinase in complex with peptide substrate and ATP analog. *EMBO J.* **16**, 5572–5581.
40. Hubbard, S. R., Wei, L., Ellis, L. & Hendrickson, W. A. (1994). Crystal structure of the tyrosine kinase domain of the human insulin receptor. *Nature*, **372**, 746–754.
41. Russo, A. A., Jeffrey, P. D. & Pavletich, N. P. (1996). Structural basis of cyclin-dependent kinase activation by phosphorylation. *Nature Struct. Biol.* **3**, 696–700.
42. De Bondt, H. L., Rosenblatt, J., Jancarik, J., Jones, H. D., Morgan, D. O. & Kim, S. H. (1993). Crystal structure of cyclin-dependent kinase 2. *Nature*, **363**, 595–602.
43. Zhou, J. & Adams, J. A. (1997). Is there a catalytic base in the active site of cAMP-dependent protein kinase? *Biochemistry*, **36**, 2977–2984.
44. Valiev, M., Kawai, R., Adams, J. A. & Weare, J. H. (2003). The role of the putative catalytic base in the phosphoryl transfer reaction in a protein kinase: first-principles calculations. *J. Am. Chem. Soc.* **125**, 9926–9927.
45. Manning, G., Whyte, D. B., Martinez, R., Hunter, T. & Sudarsanam, S. (2002). The protein kinase complement of the human genome. *Science*, **298**, 1912–1934.
46. Nolen, B., Yun, C. Y., Wong, C. F., McCammon, J. A., Fu, X. D. & Ghosh, G. (2001). The structure of Sky1p reveals a novel mechanism for constitutive activity. *Nature Struct. Biol.* **8**, 176–183.
47. Yonemoto, W., Garrod, S. M., Bell, S. M. & Taylor, S. S. (1993). Identification of phosphorylation sites in the recombinant catalytic subunit of cAMP-dependent protein kinase. *J. Biol. Chem.* **268**, 18626–18632.
48. Herberg, F. W., Bell, S. M. & Taylor, S. S. (1993). Expression of the catalytic subunit of cAMP-dependent protein kinase in *Escherichia coli*: multiple isozymes reflect different phosphorylation states. *Protein Eng.* **6**, 771–777.
49. Zheng, J. H., Knighton, D. R., Xuong, N. H., Parello, J., Taylor, S. S. & Sowadski, J. M. (1992). Crystallization studies of the catalytic subunit of cAMP-dependent protein kinase: crystals of murine recombinant catalytic subunit and a mutant, Cys 343-Ser, diffract to 2.7 Å resolution. *Acta Crystallog. sect. B*, **48**, 241–244.
50. Otwinowski, Z. & Minor, W. (1997). Processing of X-ray diffraction data collected in oscillation mode. *Methods Enzymol.* **276**, 307–326.
51. Brunger, A. T., Adams, P. D., Clore, G. M., DeLano, W. L., Gros, P., Grosse-Kunstleve, R. W. *et al.* (1998). Crystallography and NMR system:a new software suite for macromolecular structure determination. *Acta Crystallog. sect. D*, **54**, 905–921.
52. Sheldrick, G. M. & Schneider, T. R. (1997). SHELXL: higher resolution refinement. *Methods Enzymol.* **277**, 319–343.
53. Dauter, Z., Lanmzin, V. S. & Wilson, K. S. (1997). The benefits of atomic resolution. *Curr. Opin. Struct. Biol.* **7**, 681–688.
54. Merritt, E. A., Kuhn, P., Sarfaty, S., Erbe, J. L., Holmes, R. K. & Hol, W. G. (1998). The 1.25 Å resolution refinement of the cholera toxin B-pentamer: evidence of peptide backbone strain at the receptor-binding site. *J. Mol. Biol.* **282**, 1043–1059.
55. Merritt, E. A. (1999). Comparing anisotropic displacement parameters in protein structures. *Acta Crystallog. sect. D*, **55**, 1997–2004.
56. Cook, P. F., Neville, M. E., Jr, Vrana, K. E., Hartl, F. T. & Roskoski, R., Jr (1982). Adenosine cyclic 3′,5′-monophosphate dependent protein kinase: kinetic mechanism for the bovine skeletal muscle catalytic subunit. *Biochemistry,* **21**, 5794–5799.

Edited by I. Wilson

(Received 2 September 2003; received in revised form 18 November 2003; accepted 19 November 2003)